Title page

TITLE: Selected ginsenosides of the protopanaxdiol series are novel positive allosteric modulators of P2X7 receptors

Authors: R Helliwell[1], C Ong ShioukHuey[2], K Dhuna[2], J C Molero[1], J-M Ye[1], C C Xue[1], L Stokes[2]

[1]School of Health Sciences, Health Innovations Research Institute, RMIT University, Melbourne, Australia. [2]School of Medical Sciences, Health Innovations Research Institute, RMIT University, Melbourne, Australia.

Running title: Ginsenosides potentiate P2X7 receptors

Address for Correspondence: Dr L. Stokes, School of Medical Sciences, Health Innovations Research Institute, RMIT University, Bundoora West Campus, Bundoora VIC 3083, Australia. Email: leanne.stokes@rmit.edu.au

Author contributions:

RH, COS, KD, LS performed the research

LS, RH, JCM, CCX, and J-M Y designed the study

CCX and J-M Y contributed essential reagents

LS, COS and RH analysed the data

RH, LS and CCX wrote the manuscript.

List of non-standard abbreviations

PPD, protopanaxdiol; PPT, protopanaxtriol; HEK-hP2X7, HEK-293 cells stably expressing human P2X7; AM, acetoxymethyl.

SUMMARY

Background and purpose

P2X7 is an ATP-gated ion channel predominantly expressed in immune cells and plays a key role in inflammatory processes. Ginseng is a well-known Chinese herb with both pro- and anti-inflammatory properties where many of these actions have been ascribed to constituent ginsenosides. We performed a screen to determine if ginsenoside compounds could display pharmacological activity at P2X7 that might contribute to the reported immunomodulatory actions of ginseng.

Experimental approach

We used several assays to measure P2X7 responses; ATP-mediated dye uptake, intracellular calcium measurement and whole cell patch clamp recordings. HEK-293 cells stably expressing human P2X7 were used in addition to mouse macrophages endogenously expressing P2X7.

Key results

Four ginsenosides of the protopanaxdiol series, Rb1, Rh2, Rd and the metabolite compound K (CK) potentiated P2X7 dye uptake responses whereas other ginsenosides tested were ineffective (1 - 10μM). The potentiation was rapid in onset, required a threshold concentration of ATP (> 50 μM) and had an EC_{50} of 1.08 μM. CK markedly enhanced ATP activated P2X7 currents, likely via an extracellular site of action. One of the consequences of this potentiation effect is a sustained rise in intracellular Ca^{2+} that could account for the decrease in cell viability in mouse macrophages after a combination of 500 μM ATP and 10 μM CK that are non-toxic when applied alone.

Conclusions and implications

This study identifies selected ginsenosides as novel potent allosteric modulators of P2X7 channels that may account for some of the reported immune modulatory actions of protopanaxdiol ginsenosides *in vivo*.

INTRODUCTION

Ginseng has been used for at least 2000 years in China and other Asian countries to support vitality and a long life. In traditional Chinese medicine it is often described as a 'precious tonic' that stimulates natural resistance to infection and maintains homeostasis (Hanley *et al.*, 2012a; Kumagai *et al.*, 2013). It is typically extracted from the roots of *Panax ginseng* C Mayer (Asian) and *Panax quinfolious* (American) and contains a complex mixture of bioactive compounds; the most extensively studied being the 'steroid-like' dammarane triterpenoid glycosides, termed ginsenosides. Ginsenosides are further subdivided into protopanaxdiols (PPD) (examples shown in Figure 1) or protopanaxtriols (PPT) depending on the location of the sugar moieties on the dammarane carbon skeleton. Both glycosylated classes may have sugar moieties on carbon (C) 20 but protopanaxadiols can have additional sugar moieties on C-3 whereas protopanaxatriols are on C-6. The aglycones of both classes differ only in the presence of an extra hydroxyl group on C-6 in the triol (Tomasinsig *et al.*, 2008; Chotjumlong *et al.*, 2013). Ginseng is commercially available in a variety of forms (capsules, tablets, oils) where the type and amounts of constituent ginsenosides are precisely controlled. The G115 formulation tested in this study contains 4% w/w ginsenosides and is a principle constituent of Ginsana® and Gincosan® medications (Ginsana SA).

We are interested in understanding the mechanisms underlying the reported immuno-modulatory effects of ginseng/ginsenosides as they may translate into effective medications for the prevention and treatment of infective and inflammatory diseases. *In vivo* studies using ginseng formulations have been shown to protect against lung infections caused by Pseudomonas Aeruginosa improving pulmonary bacterial clearance (Song *et al.*, 1997a; Song *et al.*, 1997b; Song *et al.*, 2010) and a clinical trial demonstrated a significant reduction in the number of cases of influenza when given as an adjuvant with vaccine that correlated with increased antibody titres and NK cell activity (Scaglione *et al.*, 1996). Similar adjuvant effects have also been consistently

demonstrated with ginsenosides in vivo (Rivera *et al.*, 2005; Han *et al.*, 2013). *In vitro*, ginsenosides have been shown to either trigger or prevent apoptosis depending on cell type or the specific ginsenoside used (Ham *et al.*, 2006; Zhang *et al.*, 2008; Li *et al.*, 2012; Zhang *et al.*, 2013; Zheng *et al.*, 2014). A number of studies have also demonstrated that ginsenosides can act via either genomic Eβ or glutocorticoid receptors in the sub-micromolar range to differentially regulate angiogenesis in endothelial cells (Sengupta *et al.*, 2004; Leung *et al.*, 2006; Leung *et al.*, 2007; Leung *et al.*, 2009). However, similar to some endogenous steroids, ginsenosides have also been shown to rapidly and reversibly interact with ligand gated ion channels which points to additional non-genomic sites of action (Nah, 2014). These include both inhibitory actions on nicotinic acetylcholine receptors (Lee *et al.*, 2003), 5-HT_3 receptors (Choi *et al.*, 2003a), NMDA receptors (Kim *et al.*, 2002), $GABA_A$ receptors (Lee *et al.*, 2012), TRPV1 channels (Huang *et al.*, 2012) and potentiating actions on glycine (Noh *et al.*, 2003), $GABA_A$ receptors (Choi *et al.*, 2003b), and TRPV1 channels (Jung *et al.*, 2001).

In this study we tested the effects of ginsenosides on a subtype of ATP-gated ion channels of the P2X family, P2X7 receptors, given their important role in regulating immune cell function (Bartlett *et al.*, 2014). Studies have demonstrated P2X7 to play a role in Ca^{2+} signalling, reactive oxygen species generation and cell death pathways and regulation of such signalling pathways may control immune responses (Bartlett *et al*., 2014). We report that several glycosylated PPD ginsenosides, but not PPT ginsenosides, appear to be positive allosteric modulators of the ATP activated P2X7 channel which can lead to enhanced Ca^{2+} influx and subsequent apoptosis in macrophages. Due to the relatively high expression levels of P2X7 in immune cells, this action may account for some of the reported immune modulatory actions of PPD ginsenosides *in vivo*.

MATERIALS AND METHODS

Materials

The P2X7 agonists ATP and BzATP were obtained from Sigma Aldrich (Ryde, NSW Australia). P2X7 antagonists AZ-10606120 and A-438079 hydrochloride were obtained from Tocris Biosciences (Bristol, UK). ATP was prepared as a 100 mM stock in double distilled water, pH to 7.4 with NaOH and was stored at -80 °C until the day of experiment. AZ-10606120 and A-438079 (10 mM in DMSO) were stored at -20 °C. Ginsenosides (certified as 98 % pure) were obtained from Chengdu Mansite Pharmaceutical Co Ltd (PPT, Rg1, Rg3, Rb1, Rb2, CK), Sichuan Weikeqi Biological Technology Co. Ltd, (PPD, Rf), Chengdu Biopurify Phytochemicals Ltd (Rc, Rd, Re) and Shanghai E Star Bio Technology Co Ltd (Rh1, Rh2). Each compound was prepared as a 50 mM stock in DMSO and stored at -80 °C until the day of the experiment. All ginsenoside stocks were further diluted in DMSO to 1000X final concentration so that when diluted in assay buffers the final concentration of DMSO was 0.1%.

Cell Culture

HEK-293 cells stably transfected with the human P2X7 (standard nomenclature conforms to guidelines (Alexander *et al*., 2013)) plasmid (clone pJB3) were maintained in DMEM:F12 media (Life Technologies catalogue number 11320-033) supplemented with 10% foetal bovine serum (FBS, French origin, Bovogen, Australia), 1% Glutamax, 10 000 U. ml^{-1} penicillin and 10 mg. ml^{-1} streptomycin with selection under 400 μg. mL^{-1} G418 (Life Technologies). The J774 murine macrophage cell line was maintained in RPMI 1640 media supplemented with 10% FBS, 1% Glutamax, and 1% penicillin and streptomycin (Bhaskaracharya *et al.*, 2014).

Animals

Animal care and procedures were performed with permission of the local RMIT Animal Ethics Committee (approval number AEC1312) and in accordance with Australian guidelines for the use of animals. All studies involving animals are reported in accordance with the ARRIVE guidelines (Kilkenny *et al*., 2010). Adult male C57BL/6 mice were maintained in a 12h light/dark cycle and fed standard diet with water *ad libitum*. Mice were killed by CO_2 asphyxiation and peritoneal macrophages were obtained by flushing the peritoneal cavity with cold PBS (5 ml).

Dye uptake experiments

Cells were plated at 2.5 x 10^4 cells per well the day before experiments into poly-D-lysine coated 96-well plates (ThermoFisher). YOPRO-1 iodide (Life Technologies) was used as the membrane impermeant dye with a final concentration of 2 μM in low divalent buffer (145 mM NaCl, 5 mM KCl, 0.2 mM $CaCl_2$, 13 mM glucose, 10 mM HEPES, pH 7.3, osm 300-310). A Flexstation III plate reader (Molecular Devices) was used to acquire data using the following settings – excitation wavelength 490 nm, emission wavelength 520 nm and 6 reads per well. Data was analysed as slope of dye uptake or area under curve between 40 and 300 seconds using SoftMax Pro software (Molecular Devices).

Calcium measurements

HEK-293 cells were plated at 2.5 x 10^4 cells per well the day before experiments into poly-D-lysine coated 96-well plates. Cells were loaded with 1 μM Fluo-4AM calcium indicator dye in low divalent buffer for 30 minutes at 37 °C. This solution was then removed and replaced with standard extracellular assay buffer (145 mM NaCl, 5 mM KCl, 2 mM $CaCl_2$, 1mM $MgCl_2$, 13 mM glucose, 10 mM HEPES, pH 7.3). A Flexstation III plate reader was used to acquire data using the following

settings – excitation wavelength 490nm, emission wavelength 520 nm and 6 reads per well. ATP was injected automatically after 40 seconds.

J774 mouse macrophages were plated at 2.5 x 10^4 cells per well into poly-D-lysine coated 96-well plates. Cells were loaded with 2.5 μM Fura-2AM calcium indicator dye plus an equal volume of pluronic acid in HBSS buffer for a total of 30 minutes at 37°C. This loading solution was removed and replaced with standard extracellular assay buffer. A Flexstation III plate reader was used to acquire data using the following settings; excitation wavelengths 340 nm and 380 nm with an emiision wavelength of 520 nm. 6 reads per well was used and ATP (10X concentration) was injected automatically after 40 seconds.

Peritoneal macrophages were plated onto 12 mm glass coverslips at 10,000 cells per slip and cultured overnight. Macrophages were loaded with 1 μM Fluo-4AM in low divalent buffer for 30 minutes at 37 °C and then placed into a heated (36 °C) 35 mm bath chamber on a Nikon Eclipse Ti-U fluorescent microscope. Cells were continuously perfused with low divalent assay buffer by gravity feed and calcium signals measured using a CoolSnap HQ2 CCD camera recording green fluorescence at 520 nm. A time-lapse recording was generated with exposure time of 300 ms and gain of 500 controlled through NIS Elements software (Nikon Instruments). Regions of interest were drawn around 150-170 individual cells to measure fluorescence at each time point, background subtracted and the mean fluorescence value calculated.

Patch clamp electrophysiology

Stably expressing HEK-hP2X7 cells were plated onto 13-mm glass coverslips 4 – 24 hours before use. Membrane currents were recorded in the whole-cell patch clamp configuration using an EPC10 amplifier (HEKA, Lambrecht, Germany) and borosilicate glass electrodes (Clark Electromedical), resistance 3-8 MOhm when filled with standard internal solution. Cells were continually perfused by gravity feed with standard divalent buffer solution (145 mM NaCl, 5 mM KCl, 2 mM $CaCl_2$,

1mM $MgCl_2$, 13 mM glucose, 10 mM HEPES, pH 7.3) prior to seal formation and with low divalent buffer solution in the majority of the experiments. Standard internal buffer solution contained NaCl 145 mM, HEPES 10 mM, EGTA 10 mM, pH 7.3 with NaOH 10M. In certain experiments, investigating permeability changes of P2X7 channels, all cations in the external solution were substituted with the large organic cation N-methyl-D-glucamine. This solution contained NMDG 154 mM, HEPES 10 mM, Glucose 13 mM, pH 7.3 with HCl 10M. Series resistance compensation was routinely applied up to a maximum of 80% to minimize voltage errors. ATP and drugs were applied using a computer controlled fast-flow system (Bio-Logic Instruments, Claix, France) with the perfusion capillaries placed in close proximity to the cell under investigation.

Cell viability assays

Cells were plated at a density of 5 x 10^4 cells/well (50 µl) in a 96 well plate (Costar) in triplicate. Compounds (or vehicle control) were added to the plate at 2X final concentration and cells were treated for 24 hours. Cell viability was assessed using the CellTiter Glo Aqueous One solution (Promega) which was added to the wells for the last 4 hours of the experiment. Absorbance was read at 490 nm using a BMG Labtech Clariostar plate reader.

Data plot and statistical analysis

Graphs were plotted using GraphPad Prism version 6 (La Jolla, USA). Concentration-response curves were fitted using a log (agonist) vs response – variable slope (four parameter) best-fit equation. Data was analysed for statistical significance using either unpaired t-tests or one-way ANOVA with post-tests as appropriate. Significance was taken as $P<0.05$.

RESULTS

Ginsenosides increase the rate of dye uptake through activated P2X7

To establish any potential effects of ginseng on P2X7 we used a standard screening assay that relies upon the uptake of the membrane impermeant dye YOPRO-1 iodide through the P2X7-dependent permeability pathway activated with the agonist ATP (Jursik *et al.*, 2007; Bhaskaracharya *et al.*, 2014). The initial screening of compounds used an approximate EC_{50} concentration of ATP (200 μM) in order to see either potentiation or inhibition of the response. We first tested a standard formulation of ginseng known as G115 since it is one of the main formulations used in the clinic. Pre-treatment of HEK cells expressing human P2X7 (HEK-hP2X7) for 10 minutes with 100 $\mu g.ml^{-1}$ G115 enhanced the rate of ATP-induced dye uptake by around 2-fold (Figure 1A, B red trace). G115 alone did not induce dye uptake in HEK-hP2X7 cells (Supplementary Figure 1) suggesting this was not due to a non-specific effect on the cells.

G115 contains a fixed amount (4% w/w) of eight ginsenosides from both PPD and PPT chemical classes, namely Rb1, Rc, Rd, Re (PPD ginsenosides) and Rb2, Rf, Rg1, Rg2 (PPT ginsenosides). It was important to establish whether the observed effects with G115 resulted from one or more specific ginsenoside(s) in the formulation. We tested 14 purified ginsenosides in a screening assay encompassing the eight ginsenosides in G115 plus the principle intestinal metabolites Rh1, Rh2, Rg3, compound K (CK) and the two aglycones PPD and PPT. All ginsenosides were tested at a concentration of 10 μM and were added 10 minutes prior to the addition of ATP (200 μM). None of the ginsenosides directly stimulated dye uptake (Supplementary Figure 1) however, four PPD ginsenosides, Rb1, Rd, Rh2 and CK, significantly increased the rate of dye uptake after ATP addition (Figure 1C). In contrast, ginsenosides of the PPT series (labelled green in Figure 1C) had no significant effect on the ATP-induced dye uptake. The chemical structures of the four ginsenosides with effect on P2X7 are shown in Figure 1D.

A glucopyranoside sugar residue in CK is essential for rapid P2X7 potentiation

Since the PPD aglycone was ineffective in potentiating P2X7 responses at concentrations up to 50 μM (data not shown) there is an absolute requirement for at least one sugar residue in this structure. Based on our data this could be located at C-3 (Rh2) or C-20 (CK). As CK appeared to be the most potent in this assay and is one of the principle metabolites of ginseng reaching plasma concentrations of around 70 $ng.ml^{-1}$ in humans (Kim *et al.*, 2013) we focused our investigation on this ginsenoside to examine the potentiating action on P2X7 in more detail.

The potentiation of ATP responses at P2X7 by CK was also demonstrated in buffer containing physiological divalent ion concentrations (2 mM Ca^{2+}, 1 mM Mg^{2+}). Under these conditions much higher concentrations of ATP (>500 μM) are required to elicit any significant dye uptake most likely due to the actions of these divalent ions in blocking P2X7 responses (Virginio *et al.*, 1997). CK could potentiate both 0.5 mM and 3 mM ATP responses (Figure 2A). The onset of potentiation of P2X7 responses by CK was rapid with immediate effects observed following co-injection of a pre-mixed cocktail of the agonist ATP and CK (Figure 2B). The response induced by ATP and CK was solely dependent on P2X7 as it could be completely abolished by pre-treatment with either of two selective P2X7 antagonists; AZ10606120 (10 μM) and A-438079 (10 μM) (Figure 2C).

Our initial experiments suggested that CK was not a direct activator or agonist of P2X7 since CK could not directly stimulate dye uptake in HEK-hP2X7 cells (Supplementary Fig 1). The EC_{50} value of the potentiation effect of CK on hP2X7 was calculated as 1.08 μM (95% CI 0.86 μM to 1.35 μM) (Figure 3A). In contrast the aglycone PPD was ineffective at all concentrations tested (0.1 – 50 μM). To determine if CK was acting as a positive allosteric modulator of P2X7 we performed a full concentration-response curve for ATP in the absence and presence of 10 μM CK (Figure 3B). Potentiation by CK left-shifted the concentration-response curve reducing the EC_{50}

from 244 μM to 71 μM, increased the maximum ATP response, and required a threshold concentration of ATP (~50 μM), In contrast when BzATP was used as a full agonist at human P2X7 (Surprenant *et al.*, 1996), CK did not increase the maximum response but did cause a left-shift in EC_{50} from 19 μM to 4.4 μM (Figure 3B). Both leftward shifts were statistically significant ($P<0.01$).

Ginsenoside CK increases sustained calcium influx through P2X7

Due to their high permeability to calcium, P2X7 activation can result in a sustained rise in intracellular Ca^{2+} leading to either proliferation/activation or cell death, depending on the magnitude and extent of channel activation (Adinolfi *et al.*, 2005b). Therefore it was important to establish whether the ginsenoside potentiation of P2X7 responses observed in dye uptake experiments lead to physiologically relevant sustained increases in intracellular Ca^{2+} concentration. We first investigated differences in intracellular Ca^{2+} responses between HEK-hP2X7 cells and the parental HEK-293 cell line (Figure 4A) using fluo-4AM loaded cells. In both cell lines there was an initial transient rise in intracellular Ca^{2+} following ATP addition which is due to the activation of G-protein coupled P2Y receptors. However only HEK-hP2X7 cells showed an additional sustained elevation in intracellular Ca^{2+} on addition of ATP concentrations > 100 μM (Figure 4A). In the presence of ginsenoside CK, this sustained calcium response was observed with 100 μM ATP (Figure 4B, blue trace). Quantification of the changes in fluo-4 relative fluorescence units (both peak response and sustained response) show that CK significantly increases the ATP-mediated rise in intracellular Ca^{2+} only in P2X7-expressing cells (Figure 4C).

Ginsenosides are potent modulators of ATP-evoked P2X7 currents

To definitively demonstrate that PPD ginsenosides enhanced ionic flux through activated P2X7 channels we used the whole-cell patch-clamp technique and delivery of ATP -/+ ginsenosides via

an 8-channel fast flow system. Our standard patch protocol used an initial application of 200 μM ATP for 5 seconds then switching to 200 μM ATP plus ginsenoside for 5 seconds before briefly returning to ATP alone (2 seconds) prior to wash off (Figure 5A – D). Representative traces for CK, Rd, Rb1, PPD, PPT, Rg1 and Rh1 are shown. Similar to the dye uptake experiments, we observed only glycosylated PPD ginsenosides potentiated ATP responses whereas the PPD aglycone and all PPT ginsenosides had no effect at 50 μM, the highest concentration tested. The rank order of potency was CK > Rd >Rb1 with thresholds for effect around 50 nM, 0.5 μM and 10 μM respectively. These effects were rapid in onset occurring in <1 second of switching from ATP alone to ATP plus ginsenoside. Similarly the effects were rapidly reversible on wash-out of the ginsenoside in the continued presence of ATP. Consistent with the dye uptake data, the most potent ginsenoside CK did not directly activate P2X7 channels, only after prior activation with ATP (data not shown). The magnitude of potentiation was quantified by dividing the current amplitude after 5 seconds in ATP + ginsenoside by the amplitude in ATP alone immediately prior to ginsenoside addition (Figure 5E). Although all the PPD ginsenosides had a dose-dependent effect in regard to potentiating ATP evoked currents, it was not possible to demonstrate a maximal effect where further increases in ginsenoside concentration lead to no further increases in the potentiation. This was due to the fact that at higher concentrations of PPD ginsenosides the potentiating effect was so large that the cells could not be effectively voltage-clamped.

Given the rapid onset and reversibility of the potentiation it was likely that the site of interaction with P2X7 was extracellular. This was confirmed by comparing the amplitude of P2X7 currents evoked by 5 second pulses of 200 μM ATP in HEK-hP2X7 dialysed with standard pipette solution or pipette solution containing 1 μM CK for 5 minutes (Figure 6A). In both groups the amplitude of successive P2X7 currents (2 min apart) evoked by external ATP was similar; 221 ± 59 pA (n= 8) and 264 ± 48 pA (n=3) respectively (P>0.05, unpaired t –test). To confirm that the HEK-hP2X7 cells containing intracellular CK pipette solution were still responsive to extracellular CK,

500 nM CK was applied in addition to ATP for the fifth pulse (Figure 6A, open triangles) and compared to a fifth successive pulse of ATP alone in the control group. The ATP-evoked current in the presence of CK was 1953 ± 552 pA (n = 3), significantly larger than after ATP alone, 261 ± 82 pA (n =6 cells, $P<0.05$, unpaired t-test).

To confirm that the CK potentiation of the ATP activated current was solely mediated by P2X7 channels we first applied 200 μM ATP for 5 seconds followed by a 5 second addition of CK in the continued presence of ATP (Figure 6B). This resulted in a marked potentiation of the current that was almost completely and irreversibly blocked by a subsequent addition of the selective P2X7 antagonist AZ10606120 (10 μM; 92.6 ± 2% inhibition, n=4 cells) in the continued presence of CK and ATP (Figure 6B).

Ginsenoside CK does not induce an immediate permeability shift to large cations

The fact that PPD ginsenosides accelerated YO-PRO dye uptake in the presence of ATP might suggest that an underlying increase in the permeability of P2X7 channels to large molecular weight cations is associated with the potentiating action of ginsenosides. To investigate this possibility cells were bathed in a solution that contained NMDG as the only extracellular cation and dialysed with standard 145 mM NaCl-containing internal solution. Under these conditions, we applied 500 msec voltage ramps from -100 mV to +50 mV every 1 second. Fast application of ATP for 10 seconds evoked outward currents at all voltages positive to around -80 mV. The mean reversal potential (E_{rev}) at the end of the 10s ATP addition (Figure 7, black bar) was -81 ± 2.1 mV (n=4 cells) and the mean outward current amplitude at -30 mV was 1186 ± 416 pA. Solution containing ATP and 1 μM CK was then applied (Figure 7, hatched bar) which resulted in marked increase in the amplitude of the current at -30 mV within 2-3 seconds of addition (mean amplitude was 3667 ± 1017 pA). Hence under these conditions CK potentiated the amplitude of the outward current by around 3-fold but this was not associated with any measurable change in permeability (E_{rev} -81.3 ±

2.4 mV). This is illustrated in Figure 7 (inset) where representative ramps in one cell are shown at the end of the first 10s addition of ATP (ATP Ramp) and 2-3s after the subsequent addition of ATP + 1 μM CK (ATP + CK Ramp). In the continued presence of ATP + 1 μM CK there was a progressive positive shift in E_{rev} which reached -74 ± 2 mV by the end of the 10s addition (Figure 7). These data suggest that permeability changes do not contribute to the fast potentiation of the P2X7-mediated current after CK addition.

Potentiation of P2X7 by ginsenoside CK is not dependent on cations or membrane voltage

We further used patch clamp recordings of HEK-hP2X7 cells to determine whether the presence of extracellular divalent cations (Ca^{2+}, Mg^{2+}) could interact with potentiation of the ATP response. The degree of potentiation of ATP-evoked inward currents was similar in standard extracellular solution (2 mM Ca^{2+}) although a higher concentration of ATP was required; 1 mM rather than 200 μM in 0.2 mM external Ca^{2+} solution (Figure 8A). There was no voltage-dependence to the effect of CK as demonstrated by linear I-V relationships for ATP or ATP in the presence of CK (Figure 8B).

Ginsenoside CK potentiates endogenous P2X7 responses in mouse macrophages

We next established whether similar effects of the ginsenoside CK on endogenous P2X7 could be demonstrated in mouse macrophages. We determined that CK could potentiate mouse P2X7 expressed in HEK-293 cells (Supplementary Figure 2) thus ruling out a species-specific effect of ginsenosides. The EC_{50} value for CK potentiation of mouse P2X7 was 0.45 μM (Supplementary Figure 2), similar to the CK effect on human P2X7. Using the J774 mouse macrophage cell line (Figure 9A) and primary mouse peritoneal macrophages (Figure 9B) we demonstrated enhanced sustained intracellular calcium responses to 500 μM ATP in the presence of 10 μM CK compared to 500 μM ATP alone. Furthermore, patch clamp recordings from individual macrophages revealed

a similar rapid onset of potentiation of ATP-mediated inward currents in J774 and peritoneal macrophages (Figure 9C).

Finally, we investigated whether this potentiation of ATP-induced responses could translate to a significant downstream functional effect such as induction of apoptotic cell death. We used J774 macrophages and treated them with either CK alone (10 μM) or a non-lethal concentration of ATP (500 μM) for 24 hours. We determined any effect on cellular viability through an MTS viability assay. Neither 10 μM CK, DMSO or 500 μM ATP alone induced any detrimental effect on cell viability (n=4 experiments; Figure 10). In contrast, a high concentration of ATP (3 mM) for 24 hours could induce marked cell death resulting in a significant reduction of cell viability (to 16.7 ± 4.3 % of control, n=4). Treating J774 macrophages with a combination of 10 μM CK and previously non-lethal ATP (500 μM) together could also significantly reduce cell viability to 49.6 ± 11.3 % of control (Figure 10B).

DISCUSSION

In this study we have shown that certain ginsenosides (Rb1, Rh2, Rd and CK) markedly enhance P2X7 responses after prior activation with exogenous ATP. These effects were only manifest after previous P2X7 activation by orthostatic agonists (ATP, BzATP) and were first characterized in a HEK cell line expressing P2X7 and corroborated in a macrophage cell line (J774) and mouse peritoneal macrophages. The consequences of the interaction were increased Ca^{2+} influx and a subsequent decrease in cell viability to lower concentrations of ATP. Given the widespread distribution of P2X7 channels on immune cells and the fact that effects could be observed in the sub-micromolar range with one of the principle metabolites of ginseng CK, it is possible that this mechanism may account for some of the reported immune modulatory actions of ginseng *in vivo*.

Since the potentiation of P2X7 responses appears to be unique to glycosylated PPD ginsenosides and can be observed in the low to sub-micromolar range (EC_{50} of 0.45 – 1.08 μM), it is unlikely to be a non-specific interaction resulting from changes in membrane fluidity as has been suggested for certain ginsenoside actions reflecting the amphipathic nature of these steroid-like saponins (Attele *et al.*, 1999). In addition, the site of action is likely to be extracellular and may involve a direct interaction with the P2X7 channel since effects are not observed with intracellular application of CK (1 μM). The potentiation is rapid in onset and is rapidly reversible. However, the kinetics of onset/reversibility were not specifically addressed in this study but are at least within 1 second based on our patch clamp experiments using a 'fast' drug application system.

The potentiating effects of PPD ginsenosides on P2X7 are novel for this family of ligand-gated ion channels but do show some similarities to reported effects of ginsenosides on $GABA_A$ (Choi *et al.*, 2003b) and glycine currents (Noh *et al.*, 2003) in Xenopus oocytes. Although the concentrations of ginsenosides necessary for the observed effects were much higher on GABA and glycine channels (around 50 μM), these studies also indicated that PPD ginsenosides were more potent than PPT ginsenosides. Such studies of effects of ginsenosides on ion channels have been

extensively reviewed in (Nah 2014). One PPD ginsenoside, Rg3, was additionally found to directly activate GABA channels containing the γ2 subunit (Lee *et al.*, 2013). In our study we demonstrate that the aglycone compounds PPD and PPT were ineffective at potentiating P2X7 which points to an absolute requirement of at least one sugar residue in PPD ginsenosides. Interestingly both PPD and PPT alglycones have been shown to inhibit rather than potentiate $GABA_A$ currents (Lee *et al.*, 2012). However, we did not observe any inhibitory effects on P2X7 responses with any ginsenoside compound. Further investigations are required to determine if there are any shared structural features between the ginsenoside binding sites on P2X7 and $GABA_A$ channels. This may also apply to HERG channels as it has been reported that PPD ginsenosides were typically more effective than PPT ginsenosides in potentiating tail currents and PPT/PPD aglycones were ineffective (Choi *et al.*, 2011).

Glycosylated PPD ginsenosides, such as the principal ginseng metabolite CK, are novel potent positive allosteric modulators of human P2X7. Several other positive modulators of P2X7 have been described including clemastine, tenidap, polymixin B, and ivermectin (Sanz *et al.*, 1998; Ferrari *et al.*, 2004; Norenberg *et al.*, 2011; Nörenberg *et al.*, 2012). There are some similarities between the action of clemastine and CK on P2X7 channels in that their action is rapid (< 100ms), reversible, calcium- and voltage-independent, and uses an extracellular site. Similar to CK, modulators such as clemastine have no direct effects on P2X7 channels and required the presence of the agonist (Norenberg *et al.*, 2011). Although Norenberg *et al* reported an accelerated change in reversal potential occurring over tens of seconds, reflecting an increased rate in the permeability to $NMDG^+$ in the presence of ATP, they recognized that this cannot account for the rapid (<1 s) potentiating effect and reversibility of clemastine (Norenberg *et al.*, 2011). The most plausible explanation, which may also be applicable to PPD ginsenosides, is that such modulators increase the mean-open time of P2X7 channels. Furthermore, such a net increase in channel activation is known to accelerate pore dilation. Hence this hypothesis may reconcile our patch data which clearly

indicates that the rapid/reversible effects of ginsenosides are not associated with significant changes in permeability and our YOPRO data where ginsenosides clearly increase the rate of dye uptake.

An important consequence of the PPD ginsenoside action on P2X7 channels is enhanced sustained Ca^{2+} influx in both macrophages and HEK cells stably expressing human P2X7. The use of CK as a positive allosteric modulator of P2X7 reduces the concentration of ATP required to generate a sustained Ca^{2+} response (Figures 4, 8). Many downstream consequences of P2X7 activation have been demonstrated to depend on sustained Ca^{2+} signaling (Bartlett *et al.*, 2014). With regard to cell viability, brief additions of high concentrations of ATP (<5 min, >1 mM) can lead to a transient ‘ pseudoapoptosis’ that does not lead to cell death (Mackenzie *et al.*, 2005) or a delayed cell death occurring after a number of hours (Hanley *et al.*, 2012b). Higher concentrations of ATP and /or prolonged applications on the other hand lead to cell death within minutes due to massive Ca^{2+} influx (Mackenzie *et al.*, 2005). In contrast, lower concentrations of ATP (<1 mM) can have the opposite effect, stimulating proliferation and prolonging cell survival (Adinolfi *et al.*, 2005a). Consistent with this we have shown that enhancing Ca^{2+} influx via P2X7 in macrophages through the use of CK can effectively convert a sub-lethal dose of 500 μM ATP into a lethal concentration as measured by a significant decrease in cell viability after 24h (Figure 10). However given the fact that the timing and extent of Ca^{2+} influx via P2X7 can lead to different functional outcomes further studies are warranted with different ATP/PPD ginsenoside combinations and examination of other parameters in addition to cell viability.

In conclusion, the present study identifies selected ginsenosides as novel positive allosteric modulators of P2X7 channels. Our findings together suggest that the modulation of P2X7 may account for some of the reported immune modulatory actions of protopanaxdiol ginsenosides *in vivo*.

ACKNOWLEDGEMENTS

LS is supported by an RMIT University Vice Chancellor's Research Fellowship. RH is supported by funding from Guangdong Provincial Academy of Chinese Medical Sciences. COS was supported by a studentship from Singapore Polytechnic to visit RMIT University. KD is supported by an RMIT University PhD scholarship. We gratefully acknowledge the help of Dr Joanne Hart (RMIT University) for the provision of animal tissue.

REFERENCES

Adinolfi E, Callegari MG, Ferrari D, Bolognesi C, Minelli M, Wieckowski MR, et al. (2005a). Basal activation of the P2X7 ATP receptor elevates mitochondrial calcium and potential, increases cellular ATP levels, and promotes serum-independent growth. Molecular biology of the cell 16(7): 3260-3272.

Adinolfi E, Pizzirani C, Idzko M, Panther E, Norgauer J, Di Virgilio F, et al. (2005b). P2X(7) receptor: Death or life? Purinergic signalling 1(3): 219-227.

Alexander SPH, Benson HE, Faccenda E, Pawson AJ, Sharman JL, Spedding M, Peters JA, Harmar AJ, CGTP Collaborators (2013) The Concise Guide to Pharmacology: Ligand-gated Ion Channels. British Journal of Pharmacology 170: 1582-1606.

Attele AS, Wu JA, Yuan CS (1999). Ginseng pharmacology: multiple constituents and multiple actions. Biochemical pharmacology 58(11): 1685-1693.

Bartlett R, Stokes L, Sluyter R (2014). The P2X7 Receptor Channel: Recent Developments and the Use of P2X7 Antagonists in Models of Disease. Pharmacological Reviews 66(3): 638-675.

Bhaskaracharya A, Dao-Ung P, Jalilian I, Spildrejorde M, Skarratt KK, Fuller SJ, et al. (2014). Probenecid blocks human P2X7 receptor-induced dye uptake via a pannexin-1 independent mechanism. PLoS One 9(3): e93058.

Choi S-H, Shin T-J, Hwang S-H, Lee B-H, Kang J, Kim H-J, et al. (2011). Differential effects of ginsenoside metabolites on HERG k channel currents. J Ginseng Res 35(2): 191-199.

Choi S, Lee J-H, Oh S, Rhim H, Lee S-M, Nah S-Y (2003a). Effects of ginsenoside Rg2 on the 5-HT3A receptor-mediated ion current in Xenopus oocytes. Molecules and cells 15(1): 108-113.

Choi SE, Choi S, Lee JH, Whiting PJ, Lee SM, Nah SY (2003b). Effects of ginsenosides on GABA(A) receptor channels expressed in Xenopus oocytes. Archives of pharmacal research 26(1): 28-33.

Chotjumlong P, Bolscher JG, Nazmi K, Reutrakul V, Supanchart C, Buranaphatthana W, et al. (2013). Involvement of the P2X7 purinergic receptor and c-Jun N-terminal and extracellular signal-regulated kinases in cyclooxygenase-2 and prostaglandin E2 induction by LL-37. Journal of innate immunity 5(1): 72-83.

Ferrari D, Pizzirani C, Adinolfi E, Forchap S, Sitta B, Turchet L, et al. (2004). The Antibiotic Polymyxin B Modulates P2X7 Receptor Function. The Journal of Immunology 173(7): 4652-4660.

Ham Y-M, Lim J-H, Na H-K, Choi J-S, Park B-D, Yim H, et al. (2006). Ginsenoside-Rh2-induced mitochondrial depolarization and apoptosis are associated with reactive oxygen species- and Ca2+-mediated c-Jun NH2-terminal kinase 1 activation in HeLa cells. J Pharmacol Exp Ther 319(3): 1276-1285.

Han Y, Rhew KY (2013). Ginsenoside Rd induces protective anti-Candida albicans antibody through immunological adjuvant activity. Int Immunopharmacol 17(3): 651-657.

Hanley PJ, Kronlage M, Kirschning C, del Rey A, Di Virgilio F, Leipziger J, et al. (2012a). Transient P2X7 receptor activation triggers macrophage death independent of Toll-like receptors 2 and 4, caspase-1, and pannexin-1 proteins. J Biol Chem 287(13): 10650-10663.

Huang J, Ding L, Shi D, Hu J-H, Zhu Q-G, Gao S, et al. (2012). Transient receptor potential vanilloid-1 participates in the inhibitory effect of ginsenoside Rg1 on capsaicin-induced interleukin-8 and prostaglandin E2 production in HaCaT cells. J Pharm Pharmacol 64(2): 252-258.

Jung SY, Choi S, Ko YS, Park CS, Oh S, Koh SR, et al. (2001). Effects of ginsenosides on vanilloid receptor (VR1) channels expressed in Xenopus oocytes. Molecules and cells 12(3): 342-346.

Jursik C, Sluyter R, Georgiou JG, Fuller SJ, Wiley JS, Gu BJ (2007). A quantitative method for routine measurement of cell surface P2X7 receptor function in leucocyte subsets by two-colour time-resolved flow cytometry. J Immunol Methods 325(1-2): 67-77.

Kilkenny C, Browne W, Cuthill IC, Emerson M, Altman DG (2010). Animal research: Reporting in vivo experiments: The ARRIVE guidelines. British Journal of Pharmacology 160: 1577-1579.

Kim JS, Kim Y, Han S-H, Jeon J-Y, Hwang M, Im Y-J, et al. (2013). Development and validation of an LC-MS/MS method for determination of compound K in human plasma and clinical application. J Ginseng Res 37(1): 135-141.

Kim S, Ahn K, Oh TH, Nah S-Y, Rhim H (2002). Inhibitory effect of ginsenosides on NMDA receptor-mediated signals in rat hippocampal neurons. Biochemical and biophysical research communications 296(2): 247-254.

Kumagai S, Matsui K, Kawaguchi H, Yamashita T, Mohri T, Fujio Y, et al. (2013). Cathelicidin antimicrobial peptide inhibits fibroblast migration via P2X7 receptor signaling. Biochemical and biophysical research communications 437(4): 609-614.

Lee B-H, Choi S-H, Shin T-J, Hwang S-H, Kang J, Kim H-J, et al. (2012). Effects of Ginsenoside Metabolites on GABAA Receptor-Mediated Ion Currents. J Ginseng Res 36(1): 55-60.

Lee BH, Kim HJ, Chung L, Nah SY (2013). Ginsenoside Rg(3) regulates GABAA receptor channel activity: involvement of interaction with the gamma(2) subunit. European journal of pharmacology 705(1-3): 119-125.

Lee J-H, Jeong SM, Lee B-H, Kim D-H, Kim J-H, Kim J-I, et al. (2003). Differential effect of bovine serum albumin on ginsenoside metabolite-induced inhibition of alpha3beta4 nicotinic acetylcholine receptor expressed in Xenopus oocytes. Archives of pharmacal research 26(10): 868-873.

Leung KW, Cheung LW, Pon YL, Wong RN, Mak NK, Fan TP, et al. (2007). Ginsenoside Rb1 inhibits tube-like structure formation of endothelial cells by regulating pigment epithelium-derived factor through the oestrogen beta receptor. British journal of pharmacology 152(2): 207-215.

Leung KW, Leung FP, Mak NK, Tombran-Tink J, Huang Y, Wong RN (2009). Protopanaxadiol and protopanaxatriol bind to glucocorticoid and oestrogen receptors in endothelial cells. British journal of pharmacology 156(4): 626-637.

Leung KW, Pon YL, Wong RNS, Wong AST (2006). Ginsenoside-Rg1 induces vascular endothelial growth factor expression through the glucocorticoid receptor-related phosphatidylinositol 3-kinase/Akt and beta-catenin/T-cell factor-dependent pathway in human endothelial cells. J Biol Chem 281(47): 36280-36288.

Li W, Chu Y, Zhang L, Yin L, Li L (2012). Ginsenoside Rg1 prevents SK-N-SH neuroblastoma cell apoptosis induced by supernatant from Abeta1-40-stimulated THP-1 monocytes. Brain research bulletin 88(5): 501-506.

Mackenzie AB, Young MT, Adinolfi E, Surprenant A (2005). Pseudoapoptosis induced by brief activation of ATP-gated P2X7 receptors. The Journal of biological chemistry 280(40): 33968-33976.

Nah SY (2014). Ginseng ginsenoside pharmacology in the nervous system: involvement in the regulation of ion channels and receptors. Frontiers in physiology 5: 98.

Noh J-H, Choi S, Lee J-H, Betz H, Kim J-i, Park C-S, et al. (2003). Effects of ginsenosides on glycine receptor alpha1 channels expressed in Xenopus oocytes. Molecules and cells 15(1): 34-39.

Norenberg W, Hempel C, Urban N, Sobottka H, Illes P, Schaefer M (2011). Clemastine potentiates the human P2X7 receptor by sensitizing it to lower ATP concentrations. The Journal of biological chemistry 286(13): 11067-11081.

Nörenberg W, Sobottka H, Hempel C, Plötz T, Fischer W, Schmalzing G, et al. (2012). Positive allosteric modulation by ivermectin of human but not murine P2X7 receptors. British journal of pharmacology 167(1): 48-66.

Rivera E, Ekholm Pettersson F, Inganas M, Paulie S, Gronvik KO (2005). The Rb1 fraction of ginseng elicits a balanced Th1 and Th2 immune response. Vaccine 23(46-47): 5411-5419.

Sanz JM, Chiozzi P, Di Virgilio F (1998). Tenidap enhances P2Z/P2X7 receptor signalling in macrophages. European journal of pharmacology 355(2-3): 235-244.

Scaglione F, Cattaneo G, Alessandria M, Cogo R (1996). Efficacy and safety of the standardised Ginseng extract G115 for potentiating vaccination against the influenza syndrome and protection against the common cold [corrected]. Drugs under experimental and clinical research 22(2): 65-72.

Sengupta S, Toh SA, Sellers LA, Skepper JN, Koolwijk P, Leung HW, et al. (2004). Modulating angiogenesis: the yin and the yang in ginseng. Circulation 110(10): 1219-1225.

Song Z, Johansen HK, Faber V, Moser C, Kharazmi A, Rygaard J, et al. (1997a). Ginseng treatment reduces bacterial load and lung pathology in chronic Pseudomonas aeruginosa pneumonia in rats. Antimicrob Agents Chemother 41(5): 961-964.

Song Z, Kong KF, Wu H, Maricic N, Ramalingam B, Priestap H, et al. (2010). Panax ginseng has anti-infective activity against opportunistic pathogen Pseudomonas aeruginosa by inhibiting quorum sensing, a bacterial communication process critical for establishing infection. Phytomedicine : international journal of phytotherapy and phytopharmacology 17(13): 1040-1046.

Song ZJ, Johansen HK, Faber V, Hoiby N (1997b). Ginseng treatment enhances bacterial clearance and decreases lung pathology in athymic rats with chronic P. aeruginosa pneumonia. APMIS : acta pathologica, microbiologica, et immunologica Scandinavica 105(6): 438-444.

Surprenant A, Rassendren F, Kawashima E, North RA, Buell G (1996). The cytolytic P2Z receptor for extracellular ATP identified as a P2X receptor (P2X7). Science 272(5262): 735-738.

Tomasinsig L, Pizzirani C, Skerlavaj B, Pellegatti P, Gulinelli S, Tossi A, et al. (2008). The human cathelicidin LL-37 modulates the activities of the P2X7 receptor in a structure-dependent manner. The Journal of biological chemistry 283(45): 30471-30481.

Virginio C, Church D, North RA, Surprenant A (1997). Effects of divalent cations, protons and calmidazolium at the rat P2X7 receptor. Neuropharmacology 36(9): 1285-1294.

Zhang G, Liu A, Zhou Y, San X, Jin T, Jin Y (2008). Panax ginseng ginsenoside-Rg2 protects memory impairment via anti-apoptosis in a rat model with vascular dementia. J Ethnopharmacol 115(3): 441-448.

Zhang Y-L, Zhang R, Xu H-L, Yu X-F, Qu S-C, Sui D-Y (2013). 20(S)-protopanaxadiol triggers mitochondrial-mediated apoptosis in human lung adenocarcinoma A549 cells via inhibiting the PI3K/Akt signaling pathway. Am J Chin Med 41(5): 1137-1152.

Zheng Z-Z, Ming Y-L, Chen L-H, Zheng G-H, Liu S-S, Chen Q-X (2014). Compound K-induced apoptosis of human hepatocellular carcinoma MHCC97-H cells in vitro. Oncol Rep 32(1): 325-331.

FIGURE LEGENDS

Figure 1. G115 ginseng formulation and purified ginsenosides potentiate ATP-induced responses at the human P2X7 receptor.

(A) ATP-induced dye uptake was measured at 37 °C using YOPRO-1 (2 μM) as the membrane impermeant dye. Relative Fluorescence Units (RFU) were measured following excitation at 490 nm and emission recorded at 520 nm using a fluorescent plate reader (Flexstation III). HEK-hP2X7 cells were pre-treated with 10 or 100 μg. ml^{-1} G115 in a low divalent buffer for 10 minutes at 37 °C. ATP (200 μM) was then injected to elicit a P2X7 response. The mean of 5 individual wells is plotted. **(B)** Mean slope data (n=10-20 wells) is plotted for buffer control, ATP, or ATP in the presence of 10 or 100 μg. ml^{-1} G115. Error bars are SEM. ** denotes $P<0.001$ using ANOVA with Dunnett's multiple comparison test. **(C)** A total of 14 purified ginsenoside compounds were tested for potentiation of P2X7 responses at a concentration of 10 μM. All compounds were prepared in DMSO and were added to the low divalent buffer. Compounds were pre-incubated for 10 minutes prior to the addition of ATP (200 μM). **(D)** Chemical structures of ginsenosides with potentiating effect on human P2X7.

Figure 2. Ginsenoside CK acts rapidly to potentiate P2X7 responses and is prevented by selective antagonists.

(**A**) CK can potentiate P2X7 responses in buffer containing physiological concentrations of $CaCl_2$ and $MgCl_2$. Data is collated from 5-9 individual wells. ** represents $P<0.05$ from one-way ANOVA with Dunnett's post test. (**B**) Dye uptake plot showing co-injection of 100 μM ATP plus 10 μM CK (blue) compared with 100 μM ATP alone (black). The mean ± SEM response from 3 individual wells is plotted. (**C**) Mean data from 7-8 wells measuring ATP-induced dye uptake.

Selective antagonists AZ10606120 and A-438079 inhibit the response. ** represents P<0.05 from unpaired t-test (Welch's corrected).

Figure 3. CK acts as a positive allosteric modulator of P2X7.

(**A**) A concentration-response curve for the potentiating effect of CK. PPD is included as a control. (B) Concentration response curves were generated for ATP over the range 10 μM to 1 mM in the absence (black) and presence (blue) of 10 μM CK. Data is the mean of 5 independent experiments. (**C**) Concentration response curves were generated for BzATP over the range 1 μM to 0.3 mM in the absence (black) and presence (blue) of 10 μM CK. Error bars are SEM. Sigmoidal dose responses were fitted in GraphPad Prism.

Figure 4. CK enhances the sustained calcium response associated with hP2X7 activation.

(**A**) Intracellular Ca^{2+} responses were measured in fluo-4AM loaded HEK-hP2X7 cells or untransfected HEK-293 cells. Baseline values were recorded for 15 seconds and then ATP was applied. Increasing concentrations of ATP from 100 μM (open circles), 200 μM (black squares) to 500 μM (grey triangles) allows a sustained Ca^{2+}response to be measured in P2X7-expressing cells. (**B**) HEK-hP2X7 or untransfected HEK cells were treated with 100 μM ATP (black), 100 μM ATP + 0.1% DMSO (green) or 100 μM ATP + 10 μM CK (blue) and fluo-4 responses measured over time. (**C**) Quantitative measures of peak Ca^{2+} response (max – baseline) and sustained Ca^{2+} response (mean fluorescence between 140 seconds and 300 seconds) in both HEK-hP2X7 and HEK cells. ** indicates P<0.05 from one-way ANOVA with Dunnett's post test.

Figure 5. PPD ginsenosides rapidly and reversibly potentiate ATP–activated P2X7 currents.

HEK-hP2X7 cells were voltage clamped at -60 mV and ATP was rapidly applied for 5 seconds (black bars), followed by a 5 second application of ginsenoside + ATP (coloured bars) before

briefly returning to ATP alone for 2 seconds prior to wash off. Representative traces are shown for CK (**A**), Rd (**B**), Rb1 and PPD (**C**), PPT, Rg1, Rh1 (**D**). (**E**) Quantification of the dose-dependence of the potentiation by calculating I_2/I_1 (inset) and plotting the Ratio vs [Ginsenoside] μM. Solid symbols are PPD ginsenosides and open symbols are PPT ginsenosides. PPD and all members of the PPT series (PPT, Rg1 and Rh1) do not potentiate P2X7 currents at 50 μM.

Figure 6. CK potentiation of P2X7 currents is via an extracellular site

(**A**) One to five successive external applications of 200 μM ATP (5 second duration at 2 minute intervals) produced peak inward currents of similar amplitudes (control group, solid squares). With 1 μM CK added to the pipette solution, successive external applications of 200 μM ATP produced peak inward current amplitudes (open circles) similar to those recorded in the control group. Application of external CK (0.5 μM) with ATP at the 5th application in the test group of cells produced a significant potentiation of the peak inward current (open triangle). (**B**) A representative trace showing the rapid and irreversible block of the CK induced potentiation with the selective P2X7 antagonist AZ10606120 (AZ106). ATP (200 μM) was applied for 5 seconds (black bar) prior to the addition of ATP 200 μM plus CK 0.5μM for a further 5 seconds (hatched bar). AZ106 (10μM) was then applied in the continued presence of ATP and CK for 5 seconds (dark hatched bar) prior to wash out in ATP and CK only to assess reversibility. CK was then washed off in ATP alone for 2s (2^{nd} black bar).

Figure 7. CK potentiation does not involve a significant change in permeability to NMDG.

(**A**) Cells were bathed in $NMDG^+$ external solution and a similar drug addition protocol to that in Figure 5A, using 1 μM CK (drugs applied for 10s rather than 5s). Voltage ramps (500ms) were applied from -100 mV to +50 mV every second throughout the experiment. Typical leak – subtracted currents (inset) are shown after 10s in 200 μM ATP (ATP) and then after 2-3s in 200 μM

ATP +1 μM CK (ATP + CK). Under both conditions currents were outward at most voltages reflecting outward movement of Na^+ and negligible inward $NMDG^+$ movement. Even though there was a large potentiation of the ATP-evoked outward current in the presence of CK the reversal potential did not change significantly (Mean E_{rev} in ATP = -81 ±2.1 mV vs Mean E_{rev} in ATP + CK = – 81.3 ±2.4 mV, n=4 cells). Maintaining the cells in ATP + CK for a further 10s lead to a progressive positive shift in E_{re} reflecting a progressive increase in NMDG permeability and therefore pore dilation. Re addition of ATP alone for a further 10s did not appear to affect the progressive positive shift in E_{rev}

Figure 8. Ginsenoside CK potentiation of ATP-Evoked P2X7 currents is observed at physiological extracellular [Ca^{2+}] and is voltage-independent . (A) Using the same drug application protocol as depicted in Figure 5, CK (1 μM) potentiated ATP (1 mM) P2X7 currents in 2 mM extracellular Ca^{2+} to a similar extent as ATP-mediated P2X7 currents in 0.2 mM extracellular Ca^{2+}. Representative traces in 0.2 mM (left trace) and 2 mM extracellular Ca^{2+} (right trace) are shown and (**B**) potentiation was quantified as a ratio using the method shown in Figure 5E, inset (bar graph). The mean ratio ±S.E.M in 0.2 mM and 2 mM extracellular $Ca^{2+}$was 8.39 ± 1.4 (n=15 cells) and 12.7 ± 2.3 (n=6 cells) respectively. (**C**) Voltage ramps (1s duration) were continuously applied from -100 mV to +40 mV (every 1.25 seconds), from a holding potential of -60 mV. (**D**) Leak-subtracted ramp currents were obtained after 10s in ATP only and after 10s subsequent addition of ATP and 0.5 μM CK and plotted against voltage. Ramp current voltages are shown for typical cells in the presence of either 0.2 mM (left graph) or 2 mM extracellular Ca^{2+} (middle graph). From these ramp current/voltage relationships the ratio of current evoked after ATP + 0.5 μM CK and ATP alone was calculated at -100 mV and then at 20 mV increments up to +40 mV. For each cell the ratio was normalized to the ratio at +40 mV and the mean calculated. Open circles,

200μM ATP in 0.2mM extracellular Ca^{2+} and solid circles 1000μM ATP in 2mM extracellular Ca^{2+} (n=4, right graph).

Figure 9. CK potentiates ATP-induced calcium responses and inward currents in J774 macrophages and mouse peritoneal macrophages. (**A**) Intracellular Ca^{2+} responses were measured in Fura-2AM loaded J774 macrophages. Baseline values were taken for 15 seconds and then ATP (500 μM) was applied in the absence (black) or presence (blue) of 10 μM CK. Buffer control is shown in open circles. (**B**) Mouse peritoneal macrophages on 12 mm glass coverslips were loaded with fluo-4AM and intracellular Ca^{2+} responses measured using a CCD camera mounted on a Nikon Eclipse Ti-U microscope. ATP (500 μM) was applied in the absence (black) or presence (blue) of 10 μM CK. Buffer control is shown in grey circles. Quantitative measures of peak Ca^{2+}response (max – baseline) and sustained Ca^{2+} response (mean fluorescence between 140 seconds and 300 seconds) in peritoneal macrophages is shown. (**C**) Whole cell patch clamp recordings of J774 macrophages (top) and peritoneal macrophages (bottom) showing rapid potentiation of ATP-induced inward currents in the presence of 1 μM CK. Mean current density from 5-6 cells is displayed. ** indicates $P<0.05$ from one-way ANOVA with Dunnett's post test.

Figure 10. CK enhances the ability of ATP to cause cell death in J774 mouse macrophages. J774 cells were plated at 5 x 10^4 cells/well in triplicate in 96 well plates and treated with 0.1% DMSO, 10 μM CK, 500 μM ATP + 0.1% DMSO, 500 μM ATP + 10 μM CK or 3 mM ATP for 24 hours. CellTiter Aqueous ONE solution was added for the last 4 hours of treatment and absorbance was read at 490 nm using a BMGLabTech Clariostar plate reader. (**A**) shows cells after 18 hours of treatment and (**B**) is a representative cell viability experiment, representative of three independent experiments.

Figure 1

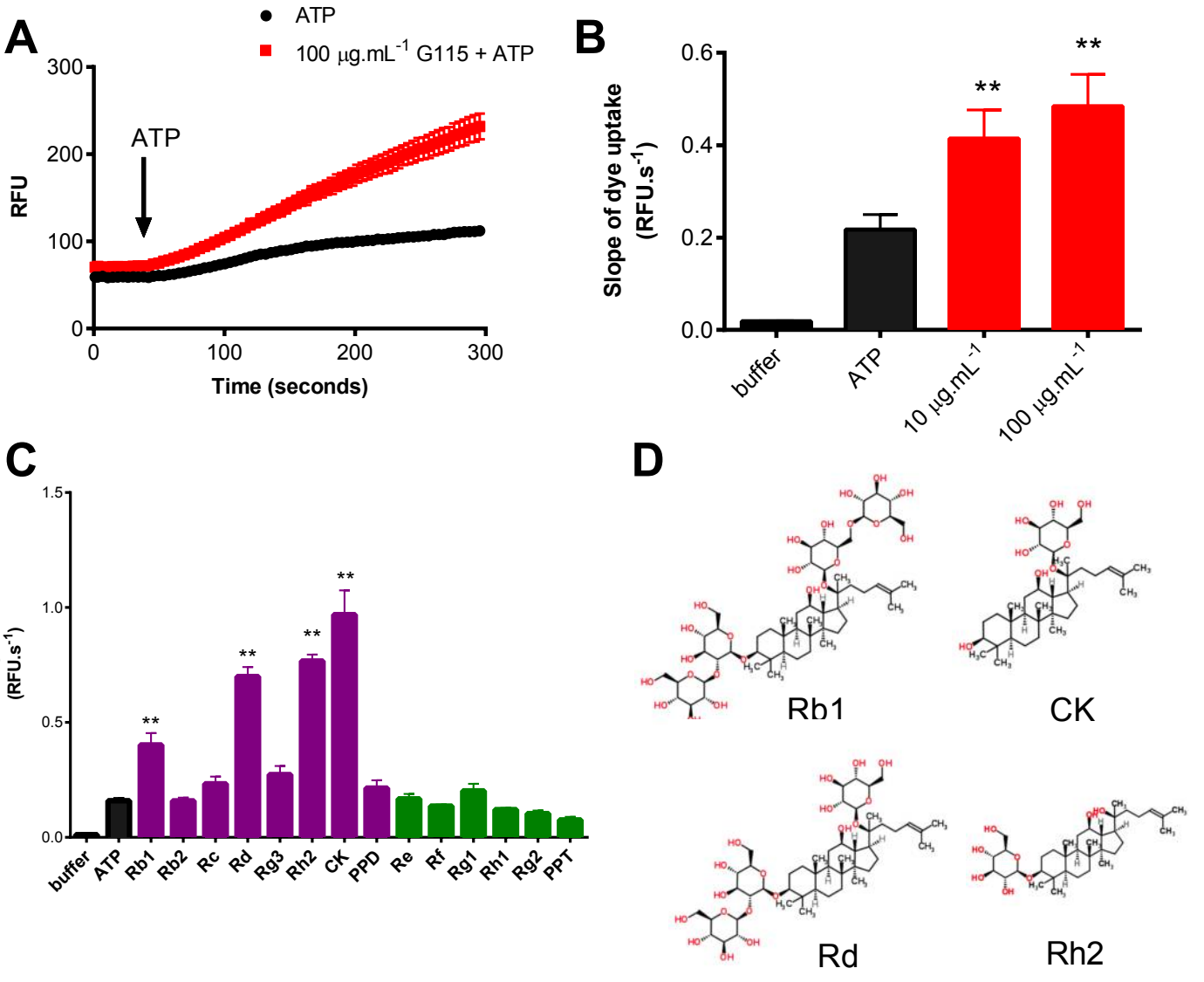
A
ATP
100 μg.mL-1 G115 + ATP
RFU
300
200
100
0
ATP
0
100
200
300
Time (seconds)
B
Slope of dye uptake (RFU.s-1)
0.6
0.4
0.2
0.0
**
**
buffer
ATP
10 μg.mL-1
100 μg.mL-1
C
Slope of dye uptake (RFU.s-1)
1.5
1.0
0.5
0.0
**
**
**
**
buffer
ATP
Rb1
Rb2
Rc
Rd
Rg3
Rh2
CK
PPD
Re
Rf
Rg1
Rh1
Rg2
PPT
D
Rb1
CK
Rd
Rh2

Figure 2

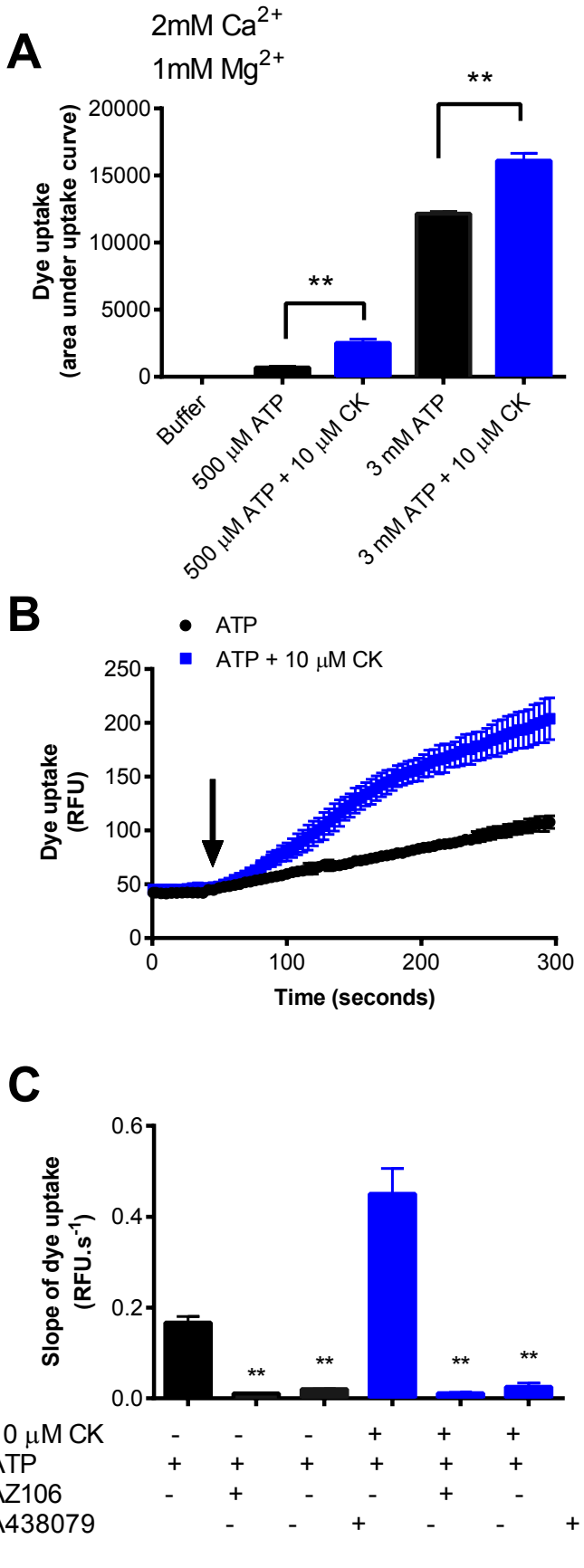
A
2mM Ca2+
1mM Mg2+
Dye uptake
(area under uptake curve)
20000
15000
10000
5000
0
**
**
Buffer
500 μM ATP
500 μM ATP + 10 μM CK
3 mM ATP
3 mM ATP + 10 μM CK
B
ATP
ATP + 10 μM CK
Dye uptake
(RFU)
250
200
150
100
50
0
0
100
200
300
Time (seconds)
C
Slope of dye uptake
(RFU.s-1)
0.6
0.4
0.2
0.0
**
**
**
**
10 μM CK - - - + + +
ATP + + + + + +
AZ106 - + - - + -
A438079 - - + - - +

Figure 3

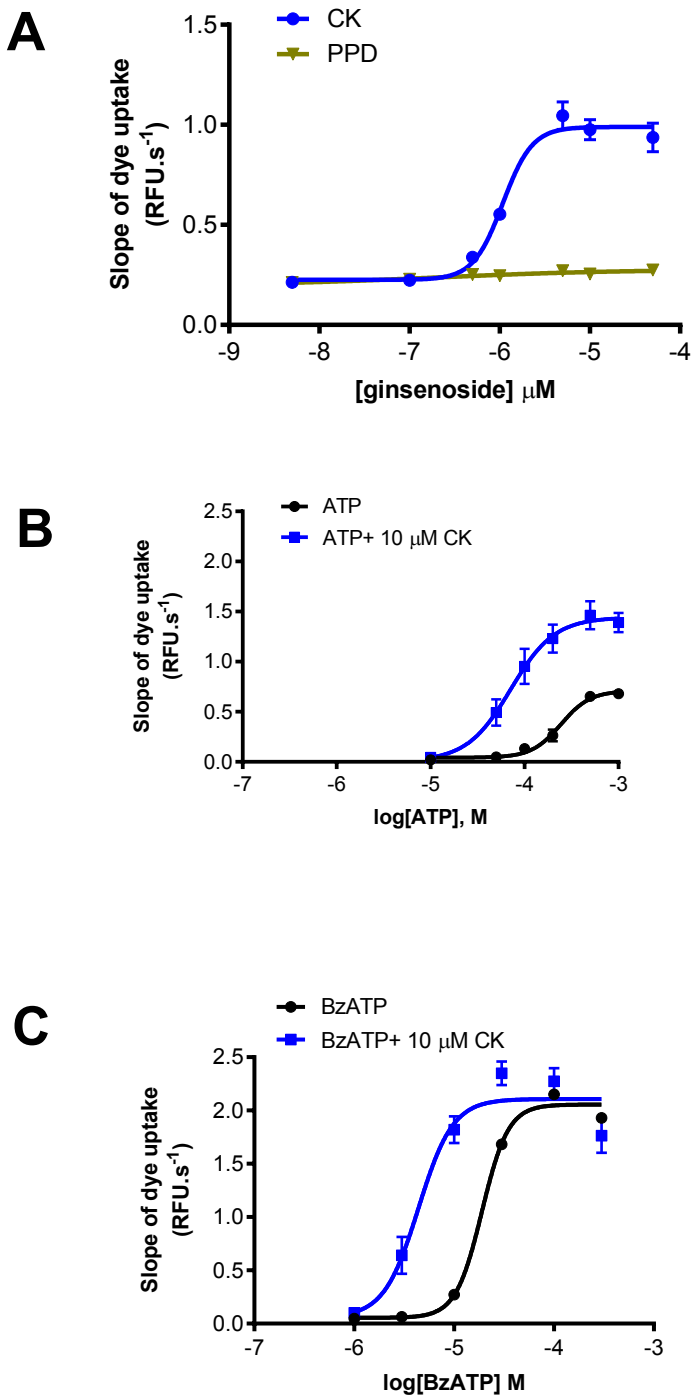
A
CK
PPD
Slope of dye uptake (RFU.s-1)
1.5
1.0
0.5
0.0
-9
-8
-7
-6
-5
-4
[ginsenoside] μM
B
ATP
ATP+ 10 μM CK
Slope of dye uptake (RFU.s-1)
2.5
2.0
1.5
1.0
0.5
0.0
-7
-6
-5
-4
-3
log[ATP], M
C
BzATP
BzATP+ 10 μM CK
Slope of dye uptake (RFU.s-1)
2.5
2.0
1.5
1.0
0.5
0.0
-7
-6
-5
-4
-3
log[BzATP] M

Figure 4

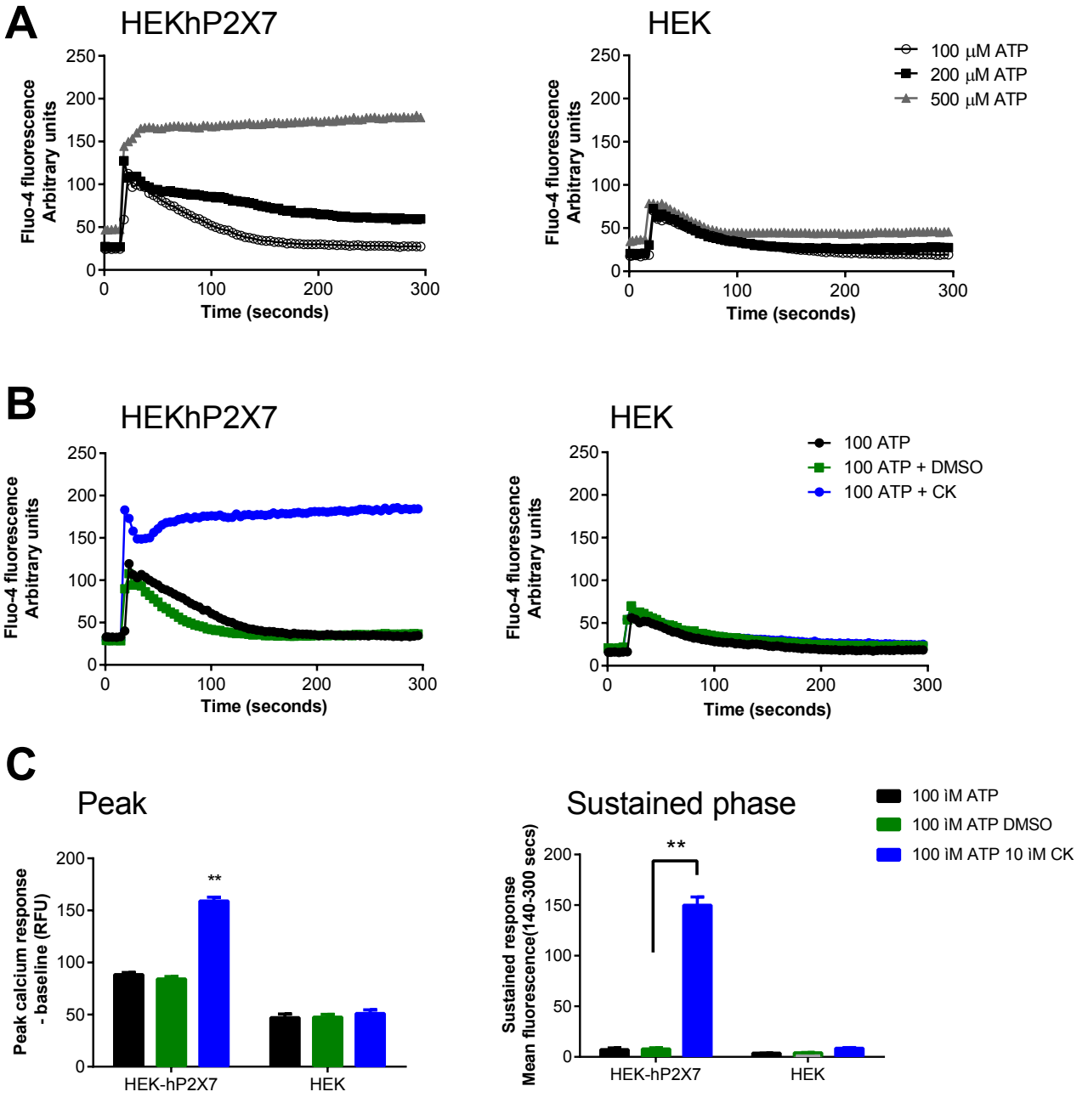
A
HEKhP2X7
HEK
100 µM ATP
200 µM ATP
500 µM ATP
Fluo-4 fluorescence Arbitrary units
Time (seconds)
B
HEKhP2X7
HEK
100 ATP
100 ATP + DMSO
100 ATP + CK
Fluo-4 fluorescence Arbitrary units
Time (seconds)
C
Peak
Peak calcium response - baseline (RFU)
HEK-hP2X7
HEK
Sustained phase
Sustained response Mean fluorescence(140-300 secs)
100 iM ATP
100 iM ATP DMSO
100 iM ATP 10 iM CK
**

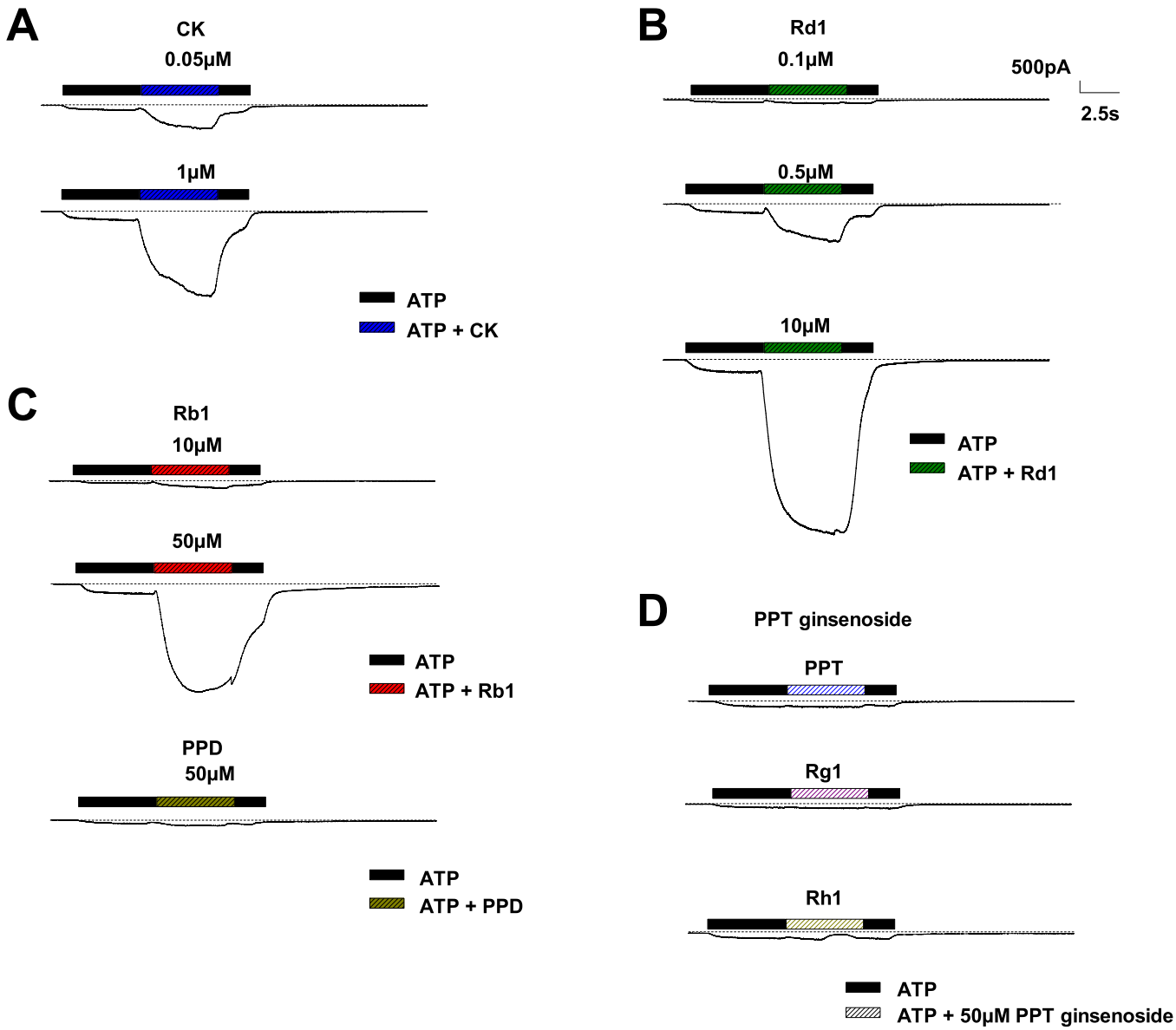
A
CK
0.05μM
1μM
ATP
ATP + CK
B
Rd1
0.1μM
500pA
2.5s
0.5μM
10μM
ATP
ATP + Rd1
C
Rb1
10μM
50μM
ATP
ATP + Rb1
PPD
50μM
ATP
ATP + PPD
D
PPT ginsenoside
PPT
Rg1
Rh1
ATP
ATP + 50μM PPT ginsenoside

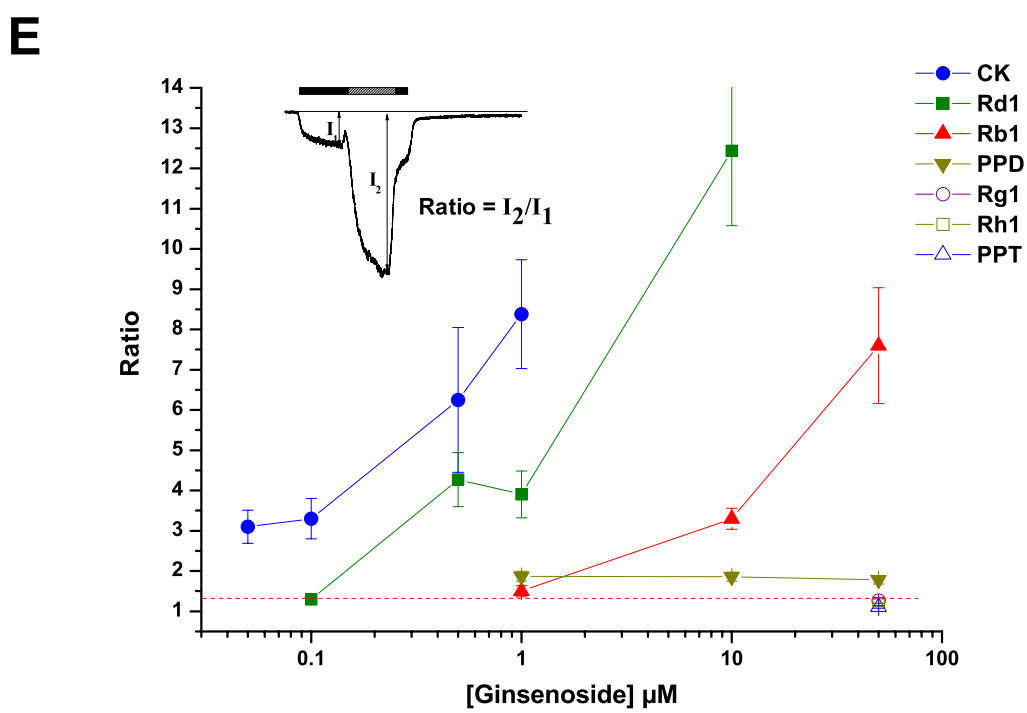
E
Ratio = I2/I1
Ratio
[Ginsenoside] μM
CK
Rd1
Rb1
PPD
Rg1
Rh1
PPT

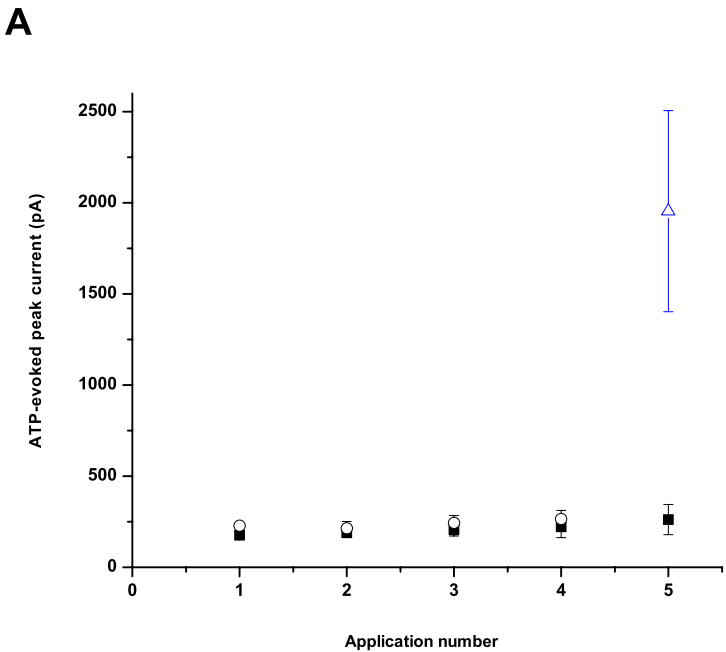
A
ATP-evoked peak current (pA)
2500
2000
1500
1000
500
0
0
1
2
3
4
5
Application number

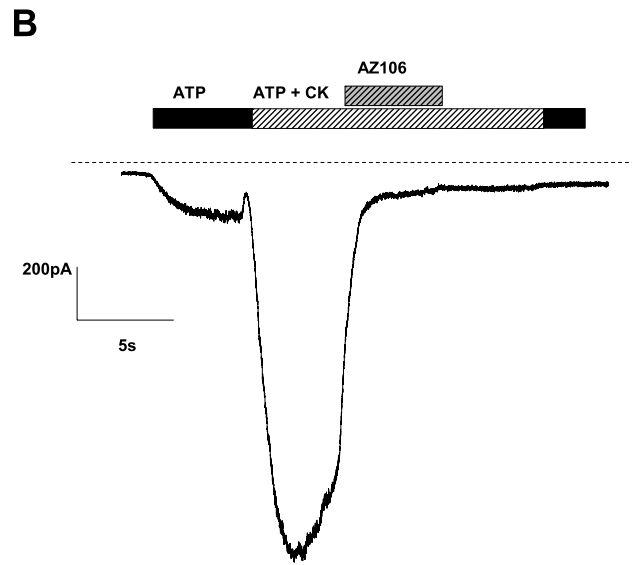
B
AZ106
ATP
ATP + CK
200pA
5s

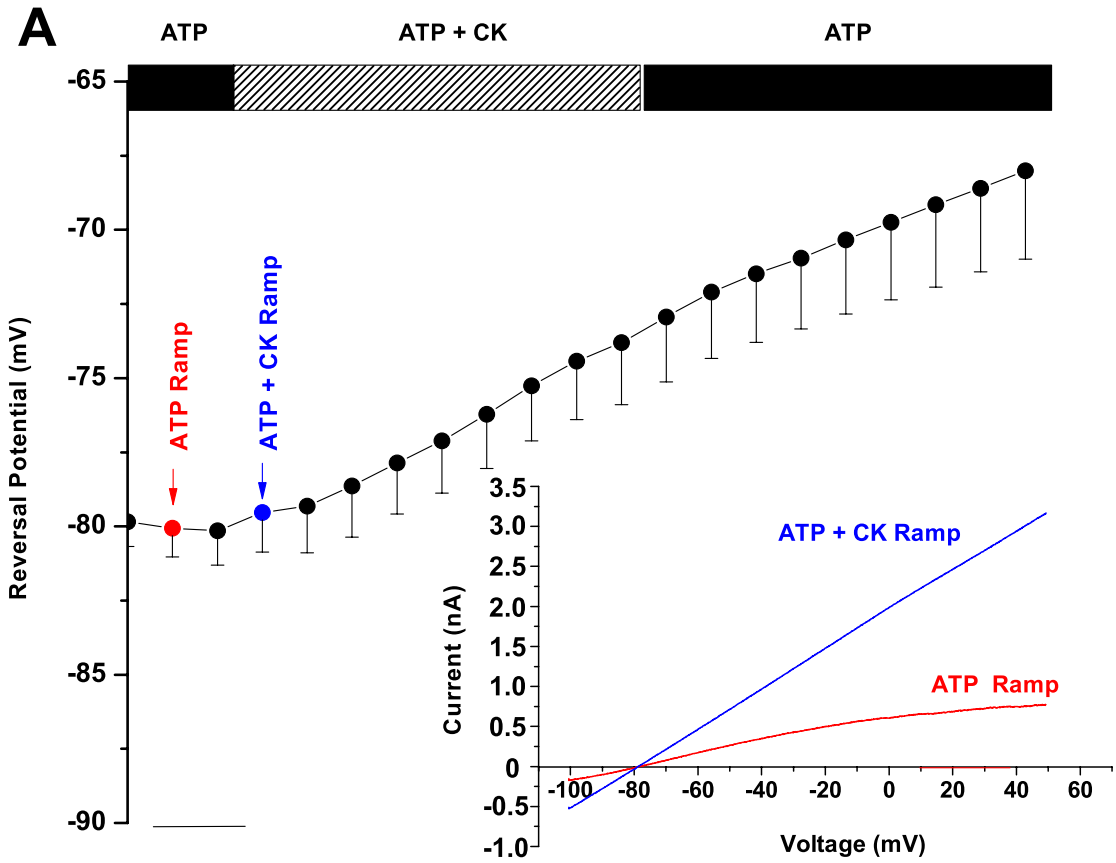
A
ATP
ATP + CK
ATP
-65
-70
-75
-80
-85
-90
Reversal Potential (mV)
ATP Ramp
ATP + CK Ramp
3.5
3.0
2.5
2.0
1.5
1.0
0.5
0
-0.5
-1.0
Current (nA)
ATP + CK Ramp
ATP Ramp
-100
-80
-60
-40
-20
0
20
40
60
Voltage (mV)

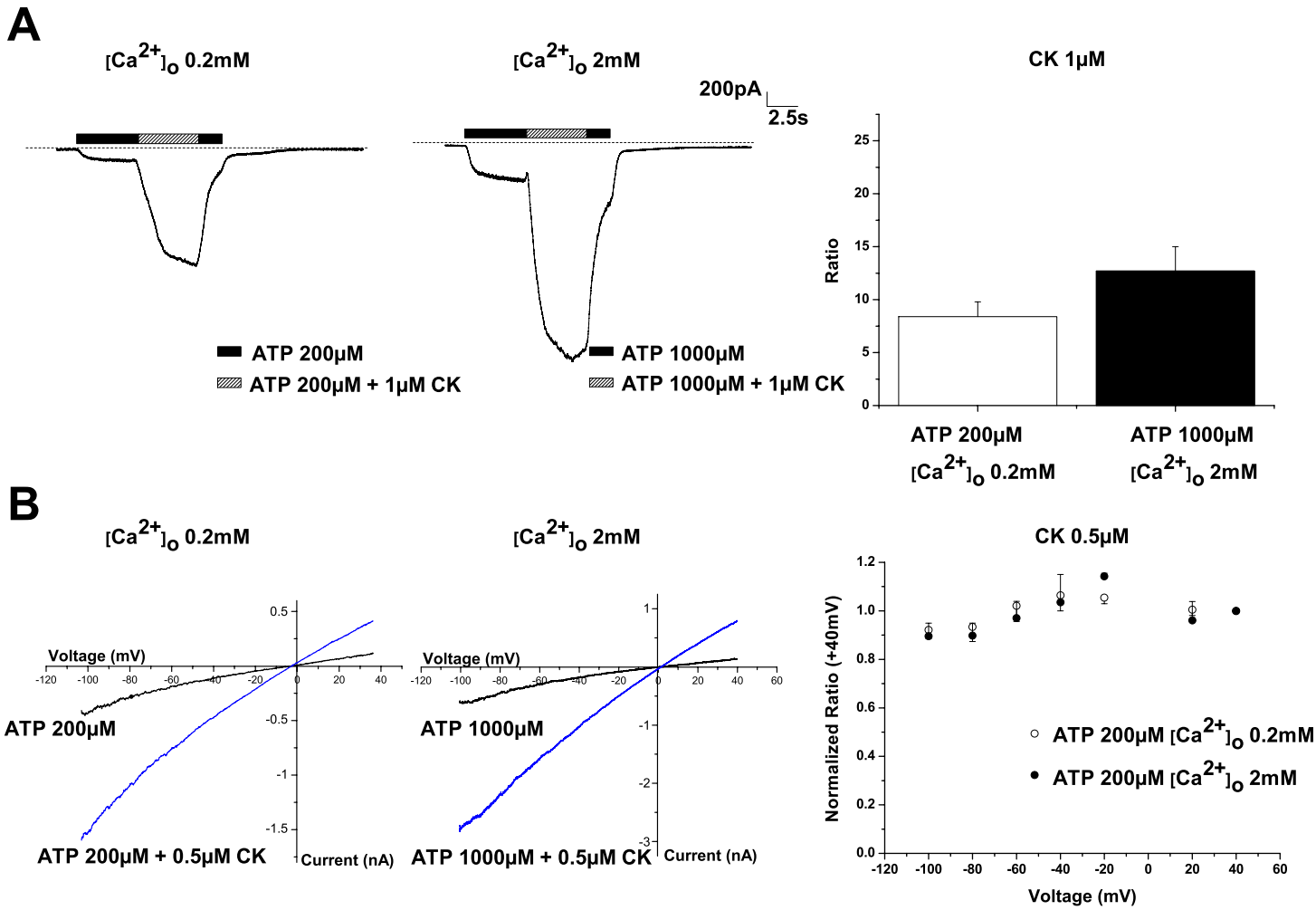
A
[Ca2+]o 0.2mM
[Ca2+]o 2mM
CK 1μM
200pA
2.5s
ATP 200μM
ATP 200μM + 1μM CK
ATP 1000μM
ATP 1000μM + 1μM CK
Ratio
ATP 200μM
[Ca2+]o 0.2mM
ATP 1000μM
[Ca2+]o 2mM
B
[Ca2+]o 0.2mM
[Ca2+]o 2mM
CK 0.5μM
Voltage (mV)
ATP 200μM
ATP 200μM + 0.5μM CK
Current (nA)
ATP 1000μM
ATP 1000μM + 0.5μM CK
Normalized Ratio (+40mV)
ATP 200μM [Ca2+]o 0.2mM
ATP 200μM [Ca2+]o 2mM
Voltage (mV)

Figure 9

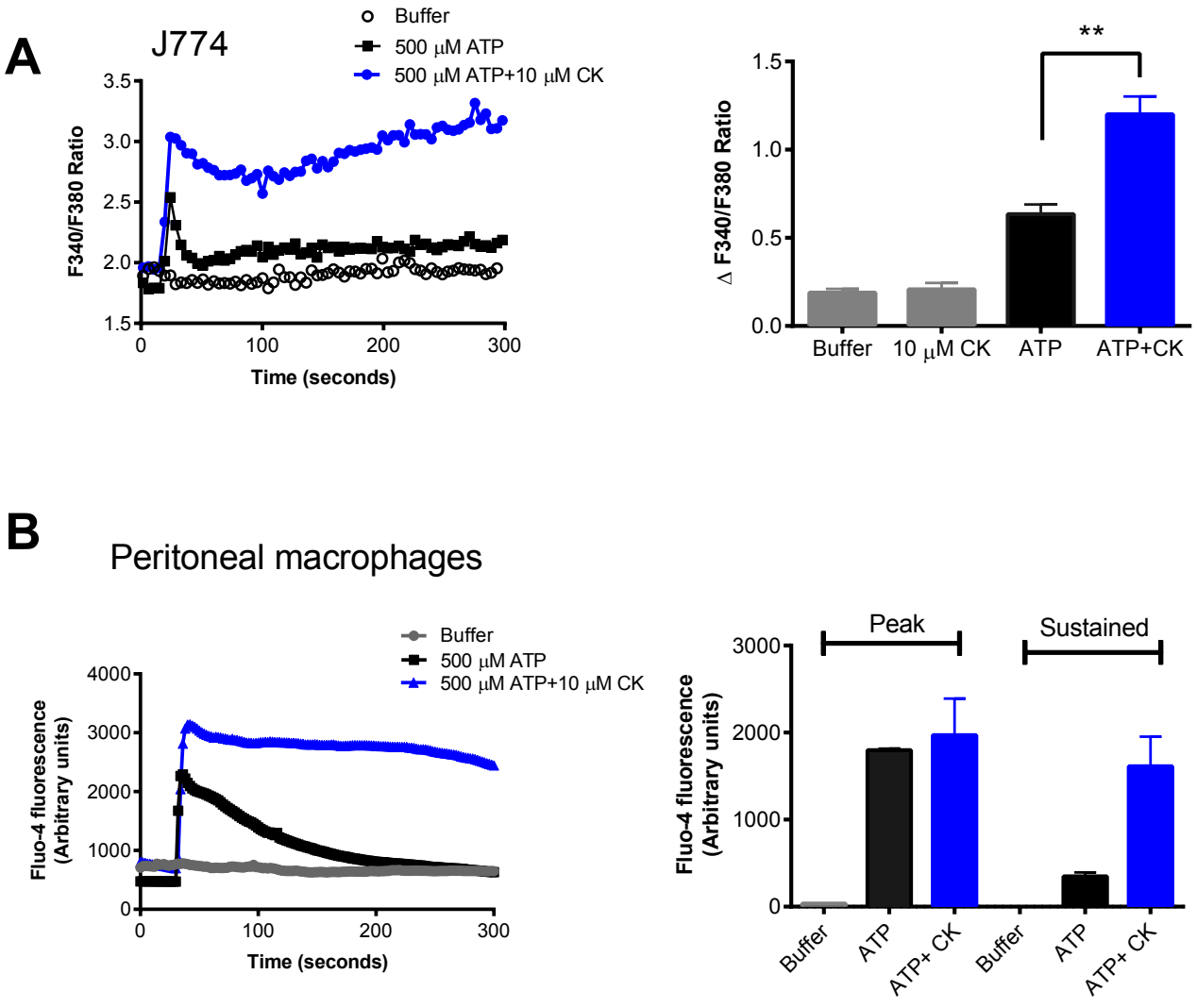
A
J774
Buffer
500 μM ATP
500 μM ATP+10 μM CK
F340/F380 Ratio
Time (seconds)
**
Δ F340/F380 Ratio
Buffer
10 μM CK
ATP
ATP+CK
B
Peritoneal macrophages
Buffer
500 μM ATP
500 μM ATP+10 μM CK
Fluo-4 fluorescence (Arbitrary units)
Time (seconds)
Peak
Sustained
Buffer
ATP
ATP+ CK
C
J774
ATP 200μM
ATP 200μM + CK1μM
100pA
2.5s
Peritoneal macrophages
ATP
ATP + 1 ?M CK
Current density (pA/pF)
J774
Per Mac

Figure 10

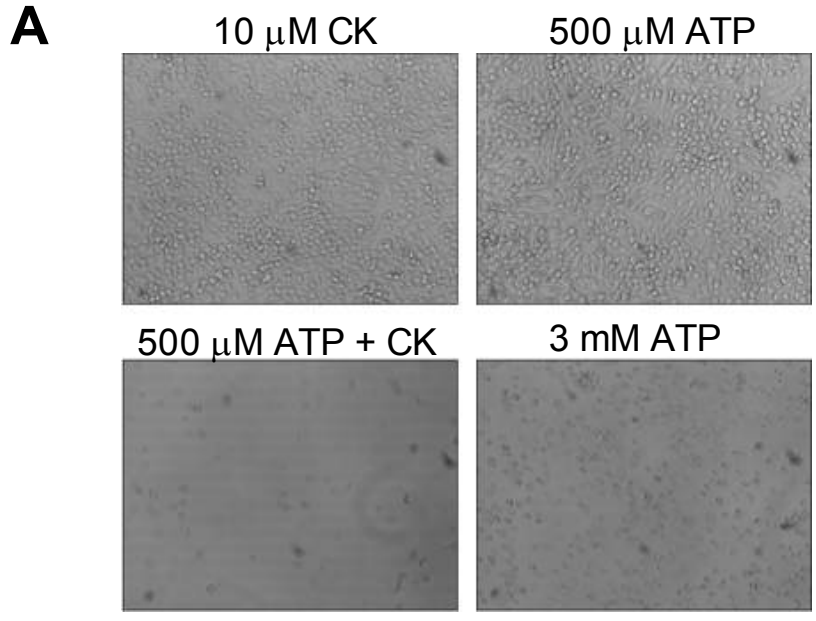
A
10 μM CK
500 μM ATP
500 μM ATP + CK
3 mM ATP
B
Cell Viability as % of control (MTS Absorbance)
120
80
40
0
**
**
DMSO - + - + - -
10 μM CK - - + - + -
ATP - - - 0.5 0.5 3mM

Supplementary Figure 1

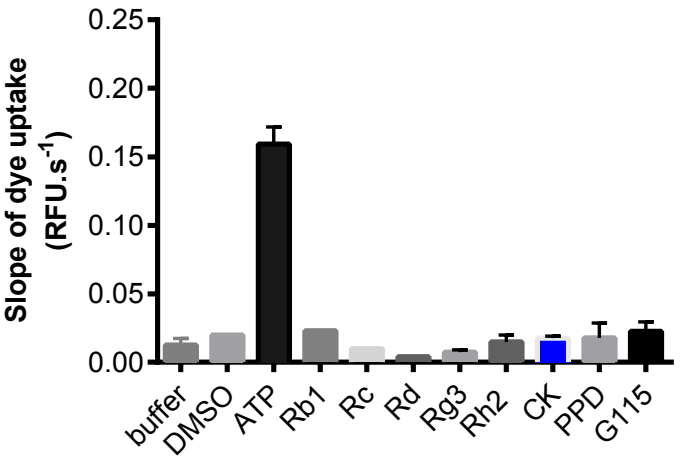

Supplementary Figure 1. Ginsenosides have no direct effect on rate of dye uptake responses in HEK-hP2X7 cells.
Dye uptake responses were measured at 37 °C using YOPRO-1 (2 ?M) as the membrane impermeant dye. Relative Fluorescence Units (RFU) were measured following excitation at 490 nm and emission recorded at 520 nm using a fluorescent plate reader (Flexstation III). HEK-hP2X7 cells were treated with ginsenosides in a low divalent buffer at 37 °C. ATP (200 ?M) was used to elicit a P2X7 response as a positive control. The mean of 5 individual wells is plotted.

Supplementary Figure 2

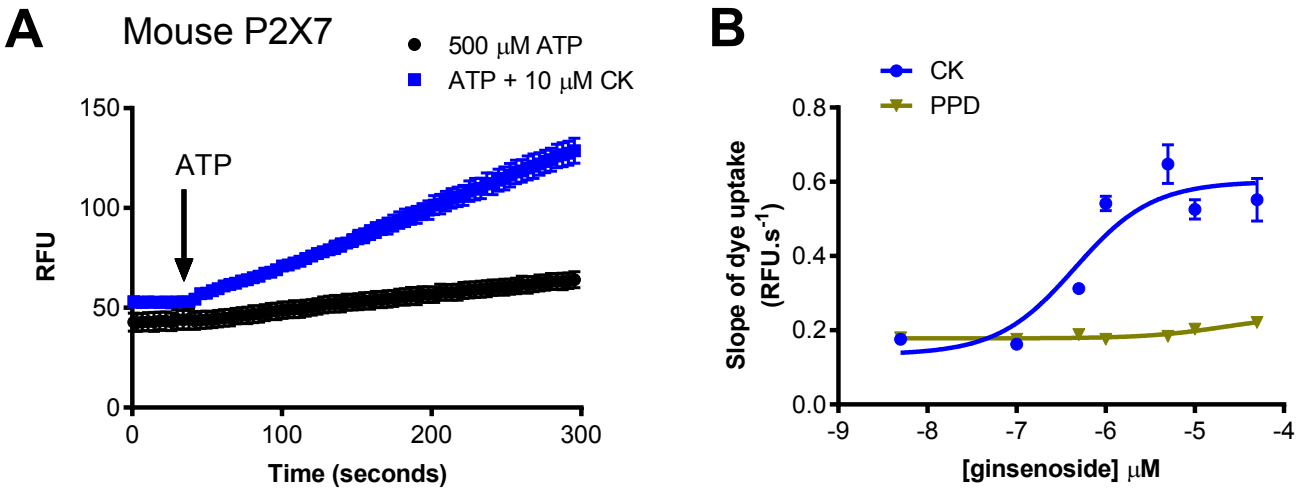

Supplementary Figure 2. CK ginsenoside potentiates ATP-induced responses at the mouse P2X7 receptor.

(A) ATP-induced dye uptake was measured at 37 °C using YOPRO-1 (2 ?M) as the membrane impermeant dye. Relative Fluorescence Units (RFU) were measured following excitation at 490 nm and emission recorded at 520 nm using a fluorescent plate reader (Flexstation III). HEK293 cells stably expressing mouse P2X7 cells were pre-treated with 10 ?M CK in a low divalent buffer for 10 minutes at 37 °C. ATP (500 ?M) was then injected to elicit a P2X7 response. The mean of 6-10 individual wells is plotted from three independent experiments. (B) A concentration-response curve for CK potentiation on mouse P2X7. Data is mean of 6 wells for each concentration.